Characterization of Tritium Transport in the Flibe-Graphite System, for In-Situ Tritium Absorption by the Fuel Elements of the Fluoride-Salt-Cooled High-Temperature Reactor (FHR)

Michael Young, Huali Wu, and Raluca Scarlat
University of Wisconsin - Madison
1500 Engineering Drive, Madison, WI 53706, USA
mcyoung4@wisc.edu, huali@wisc.edu, roscarlat@wisc.edu

ABSTRACT

Tritium control in the Fluoride-Salt-Cooled High Temperature Reactor (FHR) is an area of great interest because tritium is produced in the primary coolant (FLiBe) by neutron irradiation, and readily diffuses through metallic heat exchanger tubes at FHR operating temperatures. This paper provides an update on the tritium transport research at the University of Wisconsin - Madison in the FHR salt-fuel system.

It is expected that the matrix-graphite fuel elements in the FHR will provide a significant removable sink for tritium control. Operational data from the Molten Salt Reactor Experiment (MSRE) at Oak Ridge National Laboratory (ORNL) indicated that the graphite had a strong affinity for the tritium produced in FLiBe. Experimental data for tritium retention in graphite is available from the MSRE and from research with application to fusion systems. Data from the MSRE will be integral to benchmarking tritium retention expectation. Other experiments, which expose graphite to fixed pressures of tritium gas may not properly characterize the salt-graphite system because it may not account for conditions in the FHR primary coolant.

This paper focuses on the mechanisms for transport and retention in matrix graphite fuel within the FLiBe-matrix graphite system. The differences affecting tritium retention and kinetics between matrix graphite and nuclear graphite are proposed and discussed. In future work, benchmark models for tritium retention in graphite and experimental techniques to image tritium within graphite will be investigated.

KEYWORDS
FHR, FLiBe, Tritium Transport, Matrix Graphite

1. INTRODUCTION

The FHR is a fluoride-salt cooled reactor that combines high temperature and low pressure fluoride salt coolant with TRISO fuel dispersed in a graphite matrix that can be pressed in to pebbles, plates, or cylindrical fuel elements [1]. The Nuclear Air Brayton Combined Cycle (NACC) applied in FHR can combine a conventional Brayton cycle with a bottoming Rankine cycle to increase combined cycle efficiency to about 60% [2] and provide the capability of natural gas co-firing for power peaking.

The MSRE was first investigated in United States by ORNL in the late 1940's [3]. Due to its good chemical stability, high solubility for uranium, high volumetric heat capacity, high melting and boiling temperature, fluoride salt was chosen as the coolant in primary loop and also a potential fluid in

secondary loop. Recent MSR experience includes the Mark-1 developed by University of California - Berkeley and TMSR-SF1 designed by Chinese Academy of Science. The Mark-1 PB-FHR design is a pre-conceptual design for a small, modular FHR [4]. It is designed to produce 100 MW_e of base-load electricity and can increase to 242 MW_e output using gas co-firing. The Mk1 FHR design belongs to an Integrated Research Project (IRP) initiated by Department of Energy (DOE) in 2012 [5]. TMSR-SF1 is an experimental molten salt reactor using solid fuel. The thermal power of TMSR-SF1 is 10 MW_{th} and primary loop coolant is FLiBe. The TMSR-SF1 provides the opportunity for cooperation in collecting valuable FLiBe loop data.

The baseline primary coolant for FHR is FLiBe, which has very good heat transport and neutronics performance. However, tritium produced in FLiBe due to neutron irradiation makes the issue of tritium transport in FHR an area of interest. At the operating temperatures (427 – 704°C) of FHR, tritium readily diffuses through metallic reactor structural materials [6]. It is anticipated that tritium can be captured by graphite as it showed a high affinity for tritium in the Molten Salt Reactor Experiment (MSRE) due to its porous and crystallite structure [6].

2.   BACKGROUND

The sources and sinks for tritium in the primary coolant loop of an FHR are shown in Figure 1, and are briefly discussed in this section. There remains much variability in the design of key FHR features. Throughout this paper, the nominal point of reference is the Mk1 PB-FHR design [4]. The work discussed in this paper is generally applicable to any FHR design that uses TRISO fuel, regardless of the geometry of the fuel element – pebble fuel, plate fuel, etc.
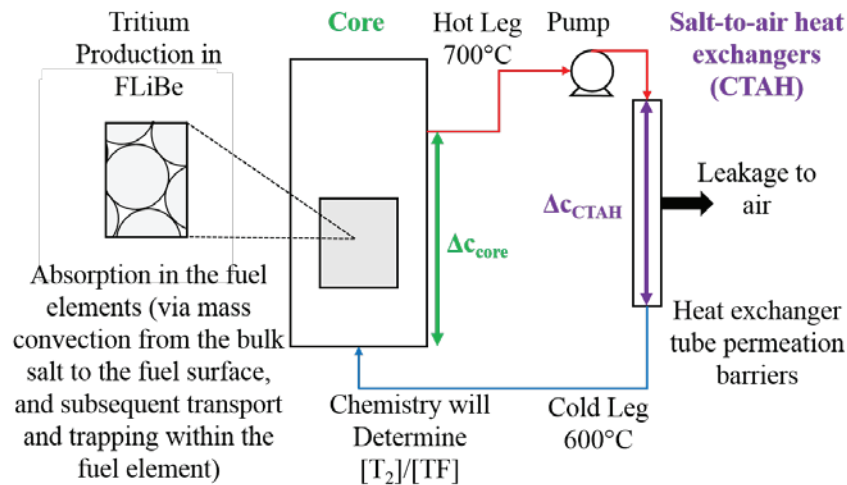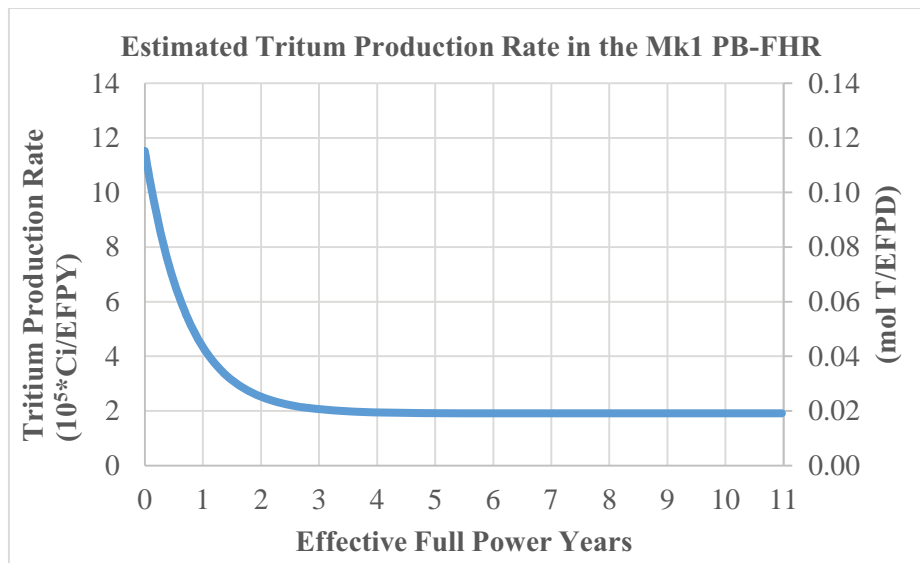

Figure 1. Tritium Sources and Sinks in the FHR Primary Coolant Loop

2.1.   Tritium Production

In the FHR, tritium (^{3}H or T) is produced due to neutron reactions on ^{6}Li, ^{7}Li, and ^{9}Be in the FLiBe salt [1]. On a per GWe basis, FHRs produce 84 mol T/yr/GWe[4] , much more than PWRs that produce 0.027 mol T/yr/GWe [7], more than HTGRs that produce 0.87 mol T/yr/GWe [8], and much less than CANDUs that produce 190 mol T/yr/GWe[1]. NRC and EPA established regulatory limits for tritium concentration in air and water effluents (0.1pCi/L for air, 1µCi/L for water)[9], but they do not specify cumulative tritium emission limits. In the absence of regulatory guidance on cumulative tritium emissions from power plants, the design goal of the FHR is to limit the tritium emissions to the emission rates of a PWR.

In the US the PWR emissions rates are reported by the NRC to be 700 Ci/year/GWe as liquid effluents (equivalent to 0.024 mol T/yr/GWe)[10], so the design goal to recover 99.9% of the tritium produced in an FHR [4].

In the first few years of operation with fresh salt, the tritium production will be higher due to a higher isotopic composition of ^{6}Li. How much higher it will be depends on the initial isotopic enrichments of Li in FLiBe, which is an expensive process, and therefore a question of economic optimization, depending on the effectiveness and availability of the tritium management systems that will be implemented in the FHR. At startup, an initial ^{6}Li percentage of 0.005 % corresponds to a tritium production rate of 0.11 mol/EFPD [11]. As the initial ^{6}Li is consumed, its consumption rate eventually equilibrates with its production rate from ^{9}Be to a ^{6}Li isotopic composition of 4 ppm [12], and the tritium production rate reaches a steady state value at 0.023 mol T/EFPD [4]. The tritium production rate against time for the Mk1 design is shown in Figure 2. This figure was modified from a figure in [1] to account for the power density and salt inventory differences between the 236 MW$_{th}$ Mk1 design and the 900 MW$_{th}$ PB-FHR design; the Mk1 design has an active core power density of 23 MW/m^3, and primary salt inventory of 47 m^3 [4].

Figure 2. Estimated Tritium Production Rate in the Mk1 PB-FHR core, as a function of Effective Full Power Years of Operation (EFPY), starting with 0.005% ^{6}Li enrichment (adapted from on neutronic calculations for the 900 MW$_{th}$ PB-FHR [1])

The initial chemical form of tritium in FLiBe is TF, as it is produced by transmutation of Li, which is present in the flibe in the chemical form of LiF. The redox control system in the salt can then lead to the formation of T$_2$ [13]. This prevents corrosion of structural steels by TF. The tradeoff in this method is that molecular tritium is highly permeable to metal heat exchangers [13]. Much of the tritium is converted to the molecular form, and a non-zero amount of TF is expected to be present.

It should be noted that the chemical form of tritium also depends on the amount of H$_2$ in the FHR system. This is important because the overall transport properties differ between HT and TF, where TF cannot permeate metal barriers [14]. With H$_2$ in the system, HT will be selectively produced; HT was shown to be favorably produced over TF when a helium/hydrogen gas of 1% partial pressure H$_2$ was swept over

FLiBe [14]. HT, similar to T_2, is permeable to metals at high temperature [14]. Based on the current status of the FHR design, it is not expected that appreciable quantities of H_2 will be in an FHR system.

2.2. Tritium Sinks

Carbon surfaces in the FHR core are expected to provide a large area for tritium absorption. In general, there are two types of graphite materials in FHR core: nuclear graphite reflector blocks and matrix graphite pebble fuel elements. The fuel elements have a much higher surface area in contact with the salt than the reflectors and provide the potential for removal of a large portion tritium with depleted fuel elements. In the Mk1 design, fuel elements comprise of 1945 m^2 [4], whereas the inner and outer reflector represent approximately 54 m^2.

Tritium has low solubility in the FHR salt and it can rapidly diffuse through metals at high temperature [15]. Tritium permeation barriers are being considered to reduce tritium permeation through Coiled-Tube Air Heater (CTAH) tubes [4]. Without these barriers, tritium transport in the FHR system is a mass-convection limited process [14]. At the system level, tritium production in the core, T_2 and TF speciation [16], and permeation through the heat exchangers must be considered. In order to properly take these sources and sinks into account, tritium production rates, molten salt electrochemistry analysis, and permeation rates with or without barriers will require detailed modeling.

Due to the solubility of tritium in water, it is a practical way to dilute tritium or titrated water by once-through cooling water system in water cooled reactor[17]. In HTGR design, tritium also can be removed by the purification system which used to remove undesirable impurities enter the coolant both by absorption or created during operation[17]. For molten salt reactor, tritium management is likely to be achieved through a joint system with salt chemical control on a side-stream of salt. The MSRE program applied an intermediate coolant which has high solubility for tritium and then tritium was collected using a gas purge system[18]. MSRE program also proposed another tritium recovery method which is to bubble inert gas (like helium) through intermediate salt coolant or even primary loop to take any dissolved gas and collected from a side stream of the salt[19].

All the methods mentioned above can be regarded as a passive way. A positive way to prevent tritium release through structural material is tritium barriers, such as metallic and ceramic barriers, which should be able to survive the same in-core environment as the base structural material[1]. The baseline design in Mark-1 applies aluminized coating on heat exchanger tubes and manifold pipes[4]. Besides the above designs, double-wall heat exchangers and membrane separator which employ tritium perm-selective nanoporous membranes can also be used to prevent tritium release to the environment. As indicated and discussed in section 2.2, large graphite surface area can provide an effective sink for tritium, which makes fuel elements, reflector pebbles can be potential tritium sinks. The following sections in the paper discussed the possibility and potential of fuel element as tritium sink for FHR.

3. TRITIUM ABSORPTION IN FHR FUEL ELEMENTS

In order to evaluate the effectiveness of the fuel elements as a tritium sink, we need to know the maximum hydrogen absorption capacity of the graphite fuel elements, and the mass transport rate from the salt into the graphite. Neither of them is well characterized for the matrix graphite material. Posing the question backwards, we can calculate a desired T/C loading at the end of the fuel life.

Assuming a tritium absorption rate in the fuel elements and graphite reflector pebbles equals the tritium generation rate and the residence time of a fuel element in the core, and the parameters given in Table I, we calculate the tritium concentration in the fuel element to be 2 µg T/g C. If the fuel elements and graphite reflector pebbles are recirculated through the core several times before discharge at 1.4 effective

full power years, and there is tritium removal step before reintroduction to the core, then this estimated tritium per carbon loading could be lower by a factor of a few.

We cannot quantify the mass transport resistance due to diffusion within the fuel element because fundamental work for the characterization of tritium diffusion and trapping within the graphite matrix is lacking. However we can estimate the mass transfer resistance due to convection from the bulk of the coolant to the surface of the fuel elements. We perform here calculations for a pebble bed. Using the same assumptions as above, we calculate the bulk concentration of tritium in the salt that would be necessary to drive mass convection to the surface of the pebbles to be 4.10×10^{-10} mol/m^3. This is the minimum bulk concentration of tritium in the salt that will drive tritium to the surface of the pebbles at a rate that balances generation in the coolant. To this, the additional mass transport resistance of tritium into the graphite will need to be added; we do not know yet which one of these transport resistances is dominant.

Further studies of the ability of the graphite matrix fuel elements to serve as an effective in-situ tritium sink need to investigate (1) limits on the tritium retention capability of the matrix graphite, (2) transport mechanisms into the graphite fuel elements, and (3) better characterization of mass convection in the salt at the prototypical conditions in the core. The following sections provide an overview of the current state of knowledge in each of these areas.

Table I. Perfect Sink Calculation Input and Outputs based on Mk1 PB-FHR Design [4], [20]

Inputs			Inputs		
Parameter	Value	Units	Parameter	Value	Units
Salt Average Temperature	650	°C	Carbon Molecular Weight	12	g/mol
Reynolds Number	500	-	Tritium Molecular Weight	3	g/mol
Schmidt Number (v/D)	1.76E+14	-	Graphite Density	1.745E+06	g/m^3
Diffusivity (Tritium in FLiBe) [15]	3.91E-09	m^2/s	Pebble Life	1.4	yr
Pebble Diameter	0.03	m	FLiBe Inventory (Primary System)	46.82	m^3
Salt Viscosity	6.78E-03	kg/(m*s)	**Outputs**		
Salt Density	1.96E+03	kg/m^3	Mass Transfer Coefficient	3.34E-01	m/s
Steady State Tritium Production Rate	2.66E-07	mol T/s	Bulk Salt Concentration at Steady State	4.09E-10	mol T/m^3
Startup Tritium Production Rate	1.28E-06	mol T/s	Bulk Salt Concentration at Startup	1.97E-09	mol T/m^3
Number of Graphite Reflector and Fuel Pebbles in the Core	688000	-	Graphite Saturation at Steady State	2.08	μg T/g C
Pebble Surface Area	1945	m^2	Graphite Saturation at Startup	9.99	μg T/g C

3.1. Tritium Saturation in Graphite

Saturation is the limit at which graphite can no longer absorb tritium. Saturation is significant because it will define the total possible retention in the FHR pebble bed and other significant graphite sinks. Saturation conditions of tritium in graphite vary greatly by experimental condition, but a reasonable estimate is on the order of tens of wppm T/C. This indicates that the 2 wppm tritium loading at fuel discharge computed above for the Mk1 PB-FHR might be achievable, and the graphite fuel elements remain a candidate for the primary tritium sink in the FHR system.

Data on tritium saturation in nuclear graphite is available from MSRE [21], [22], fusion reactors [23]–[26], gas-cooled reactors in the UK [27], [28], and the Very High Temperature Reactor (VHTR) [29] research activities. A review of this literature is presented here and experimental values are summarized in Table II. It should be noted that experimental results vary greatly for the type of graphite and appear to be strongly dependent on porosity [21].

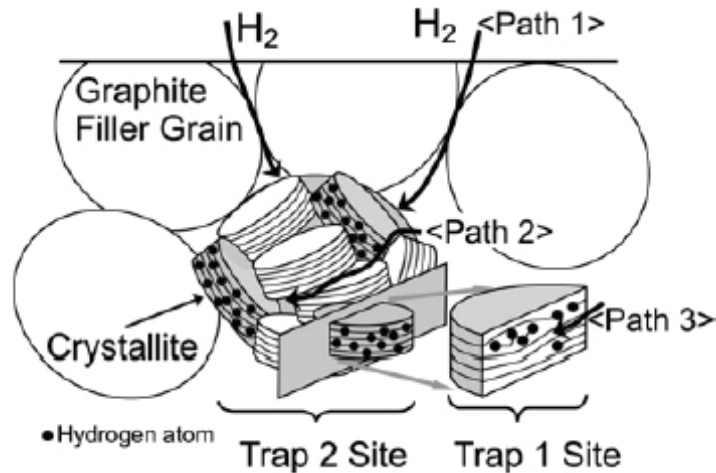**Table II. Summary of Hydrogen/Tritium Saturation in Graphite by Exposure to a Gas**

Retention	Redmond [26]	Kanashenko [25]	Atsumi [24]	Strehlow [21]	Compere [22]
Hydrogen Isotope Pressure [Pa]	133 - 101325	2500 - 90000	10000	0.14	MSRE Salt
Temperature [°C]	900 - 1500	700 - 1200	750 - 1050	750	650
Graphite Type	TSP	TSP	IG-430U	POCO	CGB
Saturation [wppm]	2.5 - 17.5	12.5 - 55	15 - 20	0.24 - 3.4	0.025 - 5

Diffusion through open pores is characterized by diffusion through the interconnected porosity of graphite and is expected to be the dominant kinetic process for tritium adsorption in graphite. Specifically, pore diffusion is assumed to occur as Knudsen diffusion [25].

Figure 3 shows the diffusion paths and trapping sites for tritium in graphite, first proposed by Kanashenko et al. [25]. Path 1 corresponds to pore diffusion, Path 2 corresponds to intragranular diffusion along crystallites, and Path 3 corresponds to intercalate diffusion between graphite lamella [24]. In FHR matrix graphite, it is expected that tritium follows Path 1 where it can then be absorbed by dangling bonds at crystallite surfaces (Trap 2 Site) [24]–[26]. This is expected because "these sites [Trap 2] are easily accessible by hydrogen because they are located on grain surfaces" whereas exceedingly high temperature is required for trans-granular diffusion to reach Trap 1 sites [25]. From Atsumi's work, the transition between pore and grain diffusion occurred around 500°C [30]. However, the hydrogen isotope partial pressures in Atsumi's work was on the order of 10's of kPa, which is relatively high compared to the tritium concentrations that will be seen in an FHR. This high partial pressure may be responsible for the discrepancy in the temperature range in identifying the dominant diffusion process from Atsumi's work [30] compared to what was seen in the MSRE.

Tritium behavior in graphite is highly temperature dependent, however, so for our recent study, we only focus on temperature range 600 °C to 750 °C and take diffusion coefficient as constant especially in modelling. Based on the pore diffusion correlation in Causey's paper [31], the relative diffusion coefficient change in this temperature range is small, around $3.6e^{-5}$. So for our recent study, we only focus on temperature range 600 °C to 750 °C and take diffusion coefficient as constant especially in modelling.

Figure 3. Tritium Diffusion Pathways and Hydrogen Trapping Sites in Graphite [24]

Work with high pressure gases suggests that there is a saturation concentration above which tritium uptake on graphite cannot proceed. Early attempts to characterize this saturation by Redmond and Walker on TSP nuclear graphite show strong dependence on the pressure of hydrogen exposed in the form of Langmuir (Temkin-type) adsorption isobars with retention on the order of 2.5 to 17.5 wppm H/C [26]. Kanashenko et al. fit this data for high temperatures assuming the concentration of Trap 1 and 2 sites of 20 and 200 appm, which yielded very accurate results, where retention was 12.5 to 55 wppm H/C [25]. Similar results were found by Atsumi on isotropic graphites corresponding to about 15 to 20 wppm H/C when exposed to 10 kPa hydrogen at relevant FHR temperature [24]. However, these results are based upon graphite exposure to high pressure gases and therefore may not be an accurate prediction for the FHR.

Strehlow exposed a variety of graphites to a tritium pressure of 0.14 Pa [21]. His results conclude an approximate expectation of a few μg T/g C (0.24 to 3.4 wppm T/C) and greatly depended on the porosity of the graphite [21]. Compere et al. analyzed 2 x 2 x 67 inches CBG graphite elements from the MSRE which yielded high surface concentrations around 5 wppm T/C and decreased to about 0.025 wppm T/C near the element center [22]. These results were also extrapolated by Compere et al. to predict that approximately 15% of all tritium produced in the MSRE was retained in graphite elements with about half trapped in the outer 1/16th-in layer of the graphite elements [22]. The discrepancies in this data will need to be resolved to understand the total possible tritium retention.

Determining a tritium saturation value applicable to the graphite in FHR is difficult due to the variation in reported data from literature and the conditions of their experiments. Experimental measurements using hydrogen isotope absorption into nuclear graphite from a high pressure gas may not reflect the same dominant phenomena as in the case of hydrogen isotope uptake into matrix graphite from a molten salt. The following conditions should be considered in evaluating the applicability of available literature data to the FHR fuel system: (1) the fluid temperature is in the 600 to 700 °C range, (2) the graphite temperature is in the 750 °C to 850 °C range, (3) the bulk concentration in the salt is expected to be in the range of 10^{-6} mol T/m^3 or above, (4) the T_2 solubility in FLiBe is in the range of 10^{-3} mol T_2/m^3 and above, depending on the T_2 partial pressure in the cover gas [15] (5) a continuous tritium generation term is present in the salt, which affects the local concentration profile and hence the driving force for mass transport, (6) matrix graphite is a composite of nuclear graphite, natural graphite and partly-graphitized carbon-material therefore the mass transport properties and the mechanisms of tritium trapping may differ

from those in nuclear graphite, (7) tritium is present in the salt as a balance of two chemical species: TF and T_2, with the ratio depending on the chemistry of the salt, (8) transport and trapping in graphite are highly affected by neutron irradiation, and the end of life neutron damage for FHR fuel element graphite matrix is expected to be in the range of 3 - 5 dpa, (9) it is unknown if the interaction between the molten salt and the matrix graphite plays any role in tritium transport and retention. Some of these conditions are further elaborated in Section 4.

3.2. Comparison with TRIDENT

Stempien et al. have created TRItium Diffusion, EvolutioN, and Transport (TRIDENT) which is the first tritium transport code to incorporate coolant chemistry, tritium speciation (TF and T_2), uptake on graphite, and corrosion reactions [16]. TRIDENT assumes that graphite pebbles saturate to levels seen by Strehlow [21]. Initial results with TRIDENT indicate that FHR graphite absorbs the majority of tritium over the initial 2 EFPD of startup and steady state concentrations in the system are achieved within 10 EFPD, at which point the production rate is equal to the release rate [32]. In such a case, the fuel elements are only a weak tritium sink in the FHR system, since it is unlikely that the fuel recirculation system would be designed with a recirculation time as short as ten days.

It is curious that TRIDENT predicts this saturation to occur at approximately 10 EFPD when the calculation summarized in Table I accounts for tritium production over the life of a fuel pebble. While it is not expected that graphite pebble fuel elements are perfect sink for tritium, the discrepancy between the saturation concentration and time to saturation needs to be resolved.

3.3. Mass Convection in FLiBe

The overall transport of tritium in the FHR pebble bed is expected to be governed by the mass transfer relation shown in Equation (1), where N_A is the molar flux, k_f is the mass transfer coefficient, and c is the concentration. Tritium convection in the core is dependent on temperature, salt potential, H_2 concentration, graphite porosity, surface damage, and saturation conditions.

The mass transfer coefficient is determined from the Wakao correlation shown in Equation (2), where D is the diffusivity (3.91e-9 m^2/s [15]), d is the pebble diameter, Sh is the Sherwood number, Sc is the Schmidt number, and Re is the Reynolds number [33]. The mass transport coefficient depends on the diffusion in FLiBe and retention kinetics in matrix graphite fuel pebbles. The diffusivity of tritium in FLiBe is dependent on temperature, salt potential, and H_2 concentration. The retention kinetics in matrix graphite are strongly dependent on temperature, porosity, surface damage, and saturation conditions.

$$N_A = k_f\left(c_{bulk} - c_{surface}\right) \qquad (1)$$

$$k_f = Sh \cdot \frac{D}{d} = \left(2 + 1.1 \cdot Sc^{\frac{1}{3}} \cdot Re_d^{0.6}\right) \cdot \frac{D}{d} \qquad (2)$$

4. CONDITIONS UNIQUE TO FHR

In FHR matrix graphite, it is expected that tritium follows Path 1 where it can then be absorbed by dangling bonds at crystallite surfaces (Trap 2 Site) [24]–[26]. This is expected because "these sites [Trap 2] are easily accessible by hydrogen because they are located on grain surfaces" whereas exceedingly high temperature is required for transgranular diffusion to reach Trap 1 sites [25]. From Atsumi's work, the transition between pore and grain diffusion occurred around 500°C [30]. However, the hydrogen isotope partial pressures in Atsumi's work was on the order of 10's of kPa, which is relatively high

compared to the tritium concentrations that will be seen in an FHR. This high partial pressure may be responsible for the discrepancy in the temperature range in identifying the dominant diffusion process from Atsumi's work [30] compared to what was seen in the MSRE.

4.1. Irradiation Effects of Diffusion and Retention

One important aspect of tritium diffusion and retention in graphite is the effect of irradiation. There are two irradiation outcomes, which are expected to affect tritium transport in graphite. The first is the decrease in intragranular diffusion coefficient over small damage levels, followed by an increase in the diffusion coefficient past approximately 0.1 - 0.2 dpa in isotropic graphites (IG-110U, IG-430U) [24]. This behavior is attributed to the saturation of Trap 2 sites and either a decrease in crystallite size or newly introduced pathways from microcracks and is shown in Figure 4 [24]. The second effect is that the retention is increased in both Trap 1 and 2 sites [24], [25]. Kanashenko et al. reported that irradiation above 1 dpa causes an increase in Trap 1 and 2 sites to 1500 and 5000 appm [25]. Atsumi found that the amount of hydrogen retained increases by a factor of about 100, where the intragranular diffusion and retention in Trap 1 sites significantly increases with irradiation as shown in Figure 5 [24].
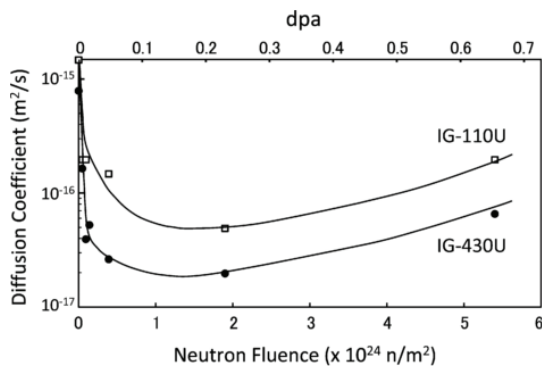

Figure 4. Granular Diffusion Coefficients with Graphite Damage [24]
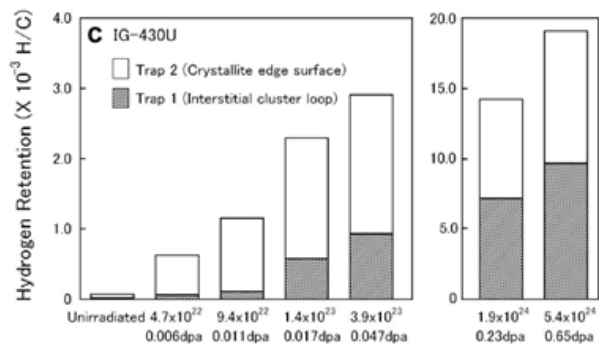
Figure 5. Hydrogen Retention with Graphite Damage [23]

In the FHR, significant damage to matrix graphite fuel elements is expected. Fast flux damage is expected to cause 3.8 dpa of damage over the 1.4 year fuel pebble life-cycle. This value is derived from a damage rate of 1.91 dpa/yr in the PB-ATHR 2009, scaled up by the power density (flux) to the Mk1 FHR design [1], [4]. The equivalent fluence, which is determined from the same scaling, is 5.17×10^{25} n/m². It is important to note that the FHR graphite damage in dpa and fluence goes well beyond the data presented in Figure 4 and Figure 5. Apart from work by Kanashenko et al. and that seen in the MSRE, which are presented above, there is little study of hydrogen retention kinetics in highly damaged graphite. Because of the similarity between the MSRE and FHR in flux [22] and fluoride salt, data from the MSRE represents the most reliable for tritium retention under neutron irradiation. It should be noted that MIT has recently conducted irradiation tests to an estimated fast fluence of 1.3×10^{24} n/m² with FLiBe and this data will soon be available [34].

4.2. Nuclear Graphite and Matrix Graphite

In order to understand the applicability of tritium retention and diffusion data obtained from the study of nuclear graphite to tritium retention and diffusion in matrix graphite, a short review of the differences between the two classes of materials, nuclear graphite and matrix graphite, is provided below. Experimentation of tritium retention on graphite, including work done by the fusion community, gas

cooled reactors and MSRE, has exclusively focused on nuclear graphite. There exists a large gap in experimentation for tritium retention in matrix graphite.

Nuclear graphite consists of coke grain (as filler) and petroleum or coal tar pitch (as binder). It can be classified to be different grades depending on coke material, density and manufacturing process [35]. Matrix graphite consists of graphite grains and graphitized binder. Germany proposed "A3 matrix" recipe in 1970's, which used natural graphite, synthetic graphite and thermosetting resin binder as the raw materials [36]. There are three types of A3 matrix depending on the composition and heat treatment, A3-3, A3-3 (1950), and A3-27. Details are shown in Table III.

Table III. Composition of Matrix graphite Material [37]

Matrix	A3-3	A3-3 (1950)	A3-27
Natural Flake Graphite	72 wt%	72 wt%	71.2 wt%
Graphitized Petroleum Coke	18 wt%	18 wt%	17.8 wt%
Nongraphitized Binder	10 wt%	10 wt%	11.0 wt%
Final Heat Treatment (°C)	1800	1950	1950

The historic grades of A3 matrix are no longer commercially available, so ORNL developed a novel matrix production method using A3 matrix composition but with modern graphite [38]. This graphite is called "GKrS", and the composition is 64 wt% natural flake milled graphite (GTI-NFM), 16 wt% synthetic graphite (SGL-KRB2000) and 20 wt% Borden Durite® SC1008 thermosetting resin.

The major difference between matrix graphite and nuclear graphite is shown in Table IV. Open porosity is percentage of reachable pores in graphite, while closed pores are pores that are not reachable. Lower heat treatment temperatures are used for matrix graphite to avoid uranium diffusion out of TRISO particles above 2273 K and creates partially graphitized binder [37], [39]. This is important for matrix graphite because this partially graphitized structure might make matrix graphite more vulnerable to irradiation, which needs to be investigated. Instruments that can be applied for graphite microstructural characterization and analysis are summarized in Table V [40]–[42].

Table IV. Difference between Nuclear Graphite and Matrix graphite

Name	Nuclear Graphite	Matrix graphite
Raw Material	Coke grain Petroleum/coal tar pitch	Graphite grain Un-graphitized binder
Heat Treatment Temperature (K)	>2973	<2273
Density (g/cm³)	1.68	1.764
Particle Size(μm)	20	11.3
Open Porosity (vol %)	14	11
Closed Porosity (vol %)	7	25

i. Property data for nuclear graphite is based on virgin graphite block from EDF UNGG Reactor [43].
ii. Property data for Matrix graphite is based on A3-27 Matrix graphite manufactured by Germany [37]

Table V. Graphite Characterization Techniques [37], [38], [42], [44], [45]

Instrument	Function
X-ray Diffraction (XRD)	Microstructure crystal structure, structure parameter
Raman Spectroscopy	Microstructure structural defect, in-plane crystallite size
Scanning Electron Microscopy (SEM)	Microstructure defect at micrometer scale
High-Resolution Transmission Electron Microscopy (HR-TEM)	Microstructure Defect at atomic scale
Optical Micrograph with MATLAB	Porosity analysis
Brunauer-Emmett-Teller (BET)	Surface area analysis
Thermogravimetric analyzer (TGA)	Graphite oxidation analysis
X-ray Photoelectron Spectroscopy (XPS)	Identify presence of element on surface examine composition

In Section 4.1, irradiation effects on tritium transport are discussed in detail from diffusion mechanism point of view. Here, irradiation caused graphite microstructure change is presented. Irradiation induces microstructural changes, including swelling and crack-closing [41]. When neutrons impinge on graphite lattice, carbon atoms are displaced from their equilibrium positions, leaving a lattice vacancy and an interstitial carbon atom. The interstitial defect will cause crystallite growth perpendicular to the layer plane and with increasing neutron dose, coalescence of vacancies will cause a shrinkage parallel to the layer plane, which means more displacement. The graphite will begin to swell due to crystallite growth and pore generation [46].

Graphite's microstructure (defects, cracks, porosity or crystallite size) largely affects tritium diffusion and retention. Matrix graphite is expected to have less open porosity, which provide fewer places for tritium occupation. Also, the partially-graphitization of matrix graphite makes it more vulnerable to irradiation. As discussed above, irradiation may cause coalescence of vacancies and pore generation, which will adversely affect tritium retention. It is worth investigating matrix graphite characterization with the techniques provided in Table V in relation to tritium diffusion and retention mechanism.

4.3.   Molten Salt Infiltration in Graphite

In the FHR, nuclear graphite blocks and matrix graphite are submerged in FLiBe. Even though graphite has inert chemical properties, due to its porous structure, molten salt may infiltrate graphite and occupy some pores [47]. In this paper we are interested in this phenomenon because we postulate that the effect of salt infiltration on tritium transport and retention should be considered.

From experiments performed by ORNL in the 1960's using molten salt fuel (LiF-BeF-UF$_4$) and "impervious" graphite rod (1/2 in diameter and 3/16 in diameter) at 1300°F for one year contact in a pump loop, graphite showed uranium and beryllium concentration of about 20 and 100 appm respectively. Figure 6 gives uranium and beryllium penetration results in graphite rods. It shows that given enough time, molten salt fuel can diffuse to the centerline of graphite rod. Also it indicated that there are no chemical interactions (oxidation or carbon dissolution) between molten salt fuel and graphite [48]. Although reports and experiments indicate molten salt shows good compatibility for nuclear graphite, it is still important to understand its compatibility with matrix graphite.
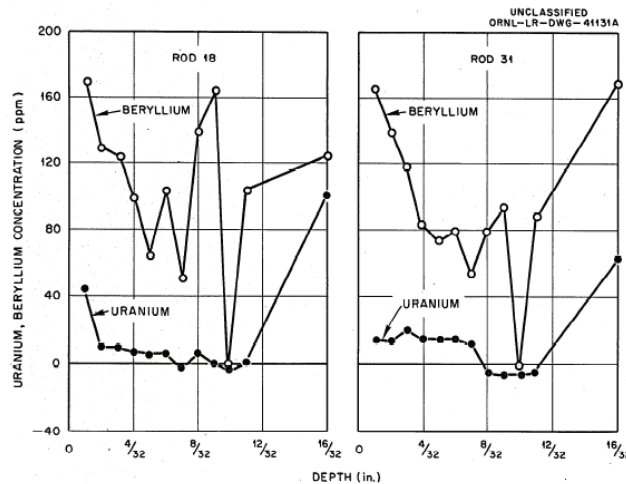

Figure 6. Penetration of Impervious graphite with LiF, BeF$_2$, UF$_4$ [48]

ORNL also investigated a method which used mercury under 452 psig pressure at room temperature to study molten salt fuel (LiF+BeF$_2$+ThF$_4$+UF$_4$) infiltration into graphite at 150 psig and 1300°F [47]. From the result of the experiment, molten salt fuel showed infiltration percentage range from 0.02 - 13.9 % for different grades of graphite [47]. Since historical nuclear graphite is no longer available, He ZhouTong from the Chinese Academy of Sciences studied molten salt (eutectic salt of LiF, NaF and KF) infiltration into modern nuclear graphite using the same method. Salt infiltration showed considerably dependency on the pressure [49] and different threshold pressures hold for different graphite. Neither experiments from ORNL, nor China reported the molten salt infiltration depth profiles into modern graphite.

5.   CONCLUSION

Tritium is produced in FLiBe by neutron irradiation and readily diffuses through metallic heat exchanger tubes at FHR operating temperatures. Graphite has been shown to be a significant sink for tritium in the MSRE. There is variability in data for the saturation of tritium in graphite. The idea of saturation may not apply to the FHR because a tritium flux from continuous production may cause continuous uptake.

Tritium is expected to diffuse through open pores and is the dominant kinetic process for tritium adsorption in graphite. Neutron irradiation of graphite is expected to increase the retention, but time-dependent diffusion of tritium in graphite.

To this point, experimentation of tritium retention has been limited to nuclear graphite. Since the majority of available graphite surfaces are matrix graphite fuel pebbles in the FHR, understanding how the differences between nuclear and matrix graphite affect tritium retention is important. Because matrix graphite is expected to have less open porosity, there are fewer available sites for tritium occupation. Experimentation, modeling, and imaging techniques for tritium absorption in matrix graphite is needed to determine the extent to which graphite fuel can be a sink for tritium in the FHR.

ACKNOWLEDGMENTS

REFERENCES

[1]   'Fluoride-Salt-Cooled High Temperature Reactor (FHR) Materials, Fuels and Components White Paper', University of California - Berkeley, UCBTH-12-003, (2013).
[2]   C. Andreades, R. O. Scarlat, et al., 'Reheat-Air Brayton Combined Cycle Power Conversion Design and Performance Under Nominal Ambient Conditions', *J. Eng. Gas Turbines Power*, **vol. 136**, no. June 2014, p. 062001, (2014).
[3]   M. W. Rosenthal, P. R. Kasten, et al., 'Molten-salt reactors-history, status, and potential', *Nucl. Appl. Technol.*, **vol. 8**, (1970).
[4]   C. Andreades, A. T. Cisneros, et al., 'Technical Description of the "Mark 1" Pebble-Bed Fluoride-Salt-Cooled High-Temperature Reactor (PB-FHR) Power Plant', University of California - Berkeley, UCBTH-14-002, (2014).
[5]   'Fluoride-Salt-Cooled High Temperature Reactor (FHR) Subsystems Definition, Functional Requiement Definition, and Licensing Basis Event (LBE) Identification White Paper', University of California - Berkeley, UCBTH-12-001, (2013).
[6]   R. B. Briggs, 'Tritium in molten-salt reactors', *React. Technol.*, **vol. 14**, pp. 335–352, (1972).
[7]   H. T. Peterson and D. A. Baker, 'Tritium Production, Releases and Population Doses at Nuclear Power Reactors', *Fusion Technol.*, **vol. 8**, pp. 2544–2550, (1985).
[8]   D. Yook, K. J. Lee, et al., 'Estimation of the Tritium Behavior in the Pebble Type Gas Cooled Reactor for Hydrogen Production', *J. Nucl. Sci. Technol.*, **vol. 43**, no. 12, pp. 1522–1529, (2006).
[9]   H. Ohashi and S. R. Sherman, 'Tritium Movement and Accumulation in the NGNP System Interface and Hydrogen Plant', Idaho National Laboratory, INL/EXT-07-12746, (2007).
[10]   'Frequently Asked Questions About Liquid Radioactive Releases', *Nuclear Regulation commission*. [Online]. Available: http://www.nrc.gov/reactors/operating/ops-experience/tritium/faqs.html#normal.
[11]   'Personal Correspondance with Anselmo T. Cisneros.' .
[12]   M. Fratoni and E. Greenspan, 'Neutronic Feasibility Assessment of Liquid Salt – Cooled Pebble Bed Reactors', *Nucl. Sci. Eng.*, **vol. 168**, pp. 1–22, (2011).
[13]   S. Fukada, A. Morisaki, et al., 'Control of tritium in FFHR-2 self-cooled Flibe blanket', *Fusion Eng. Des.*, **vol. 81**, no. 1–7, pp. 477–483, (2006).

[14]   A. Suzuki, T. Terai, et al., 'Tritium release behavior from Li 2 BeF 4 molten salt by permeation through structural materials', *Fusion Eng. Des.*, **vol. 52**, pp. 863–868, (2000).

[15]   P. Calderoni, P. Sharpe, et al., 'Measurement of tritium permeation in flibe (2LiF–BeF2)', *Fusion Eng. Des.*, **vol. 83**, no. 7–9, pp. 1331–1334, (2008).

[16]   J. D. Stempien, R. G. Ballinger, et al., 'The Coupled Corrosion and Tritium Challenges of Fluoride-Salt-Cooled High-Temperature Reactors', in *Proceedings of ICAPP 2014*, (2014).

[17]   B. W. Gainey, 'A Review of Tritium Behavior in HTGR Systems', General Atomics, GA-A13461, (1976).

[18]   H. G. Macpherson, 'The Molten Salt Reactor Adventure', *Nucl. Sci. Eng.*, **vol. 90**, pp. 374–380, (1985).

[19]   a Perujo and K. . Forcey, 'Tritium permeation barriers for fusion technology', *Fusion Eng. Des.*, **vol. 28**, pp. 252–257, (1995).

[20]   R. O. Scarlat, 'Design of Complex Systems to Achieve Passive Safety : Natural Circulation Cooling of Liquid Salt Pebble Bed Reactors', University of California - Berkeley, (2012).

[21]   R. A. Strehlow, 'Chemisorption of tritium on graphites at elevated temperatures', *J. Vac. Sci. Technol. A Vacuum, Surfaces, Film.*, **vol. 4**, no. 1986, p. 1183, (1986).

[22]   E. L. Compere, S. S. Kirslis, et al., 'Fission Product Behavior in the Molten Salt Reactor Experiment', Oak Ridge National Lab, ORNL-4865, (1975).

[23]   H. Atsumi, A. Muhaimin, et al., 'Hydrogen trapping in neutron-irradiated graphite', *J. Nucl. Mater.*, **vol. 386–388**, pp. 379–382, (2009).

[24]   H. Atsumi, T. Tanabe, et al., 'Hydrogen behavior in carbon and graphite before and after neutron irradiation – Trapping, diffusion and the simulation of bulk retention–', *J. Nucl. Mater.*, **vol. 417**, no. 1–3, pp. 633–636, (2011).

[25]   S. L. Kanashenko, A. E. Gorodetsky, et al., 'Hydrogen adsorption on and solubility in graphites', *J. Nucl. Mater.*, **vol. 233–237**, pp. 1207–1212, (1996).

[26]   J. P. Redmond and P. L. Walker, 'Hydrogen sorption on graphite at elevated temperatures', *J. Phys. Chem.*, **vol. 64**, no. 9, pp. 1093–1099, (1960).

[27]   R. Burcl, J. L. Gonzalez Gomez, et al., 'Characterization, Treatment and Conditioning of Radioactive Graphite from Decommissioning of Nuclear Reactors', IAEA, IAEA-TECDOC 1521, (2006).

[28]   B. J. Marsden, 'Production, Location and Retention of Tritium in Irradiated Graphite', AEAT, AEAT/RJCB/RD03510001/R02, (2001).

[29]   E. S. Kim, C. H. Oh, et al., 'Development of Tritium Permeation Analysis Code (TPAC)', (2010).

[30]   H. Atsumi, S. Tokura, et al., 'Absorption and desorption of deuterium on graphite at elevated temperatures', *J. Nucl. Mater.*, **vol. 155–157**, pp. 241–245, (1988).

[31]   R. A. Causey, 'The retention of deuterium and tritium in POCO AXF-5Q graphite', *J. Vac. Sci. Technol. A Vacuum, Surfaces, Film.*, **vol. 4**, no. 3, p. 1189, (1986).

[32]   J. D. Stempien, R. G. Ballinger, et al., 'Tritium Transport and Corrosion Modeling in the Fluoride Salt-Cooled High-Temperature Reactor', in *2014 ANS Winter Conference*, (2014).

[33]   N. Wakao, S. Kaguei, et al., 'Effect of fluid dispersion coefficients on particle-to-fluid heat transfer coefficients in packed beds', *Chem. Eng. Sci.*, **vol. 34**, no. 3, pp. 325–336, (1979).

[34]   D. Carpenter, M. Ames, et al., 'Findings of the second round of fluoride salt high temperature reactor materials irradiation tests at the MIT research reactor', in *Proceedings of ICAPP 2015*, (2015).

[35]   S. Chi and G. Kim, 'Comparison of the oxidation rate and degree of graphitization of selected IG and NBG nuclear graphite grades', *J. Nucl. Mater.*, **vol. 381**, no. 1–2, pp. 9–14, (2008).

[36] R. E. Bullock, 'All ceramic fuel elements for the high-temperature gas-cooled reactor', *High Temp. Press.*, **vol. 12**, pp. 599–633, (1980).

[37] E. Hoinkis and E. Robens, 'Surface area and porosity of unmodified graphitic matrices A3-27 and A3-3 (1950) and oxidized matrix A3-3 (1950)', *Carbon N. Y.*, **vol. 27**, no. 1, pp. 157–168, (1989).

[38] J. J. Lee, T. K. Ghosh, et al., 'Oxidation rate of graphite matrix material in the kinetic regime for VHTR air ingress accident scenarios', *J. Nucl. Mater.*, **vol. 446**, no. 1–3, pp. 38–48, (2014).

[39] R. Moormann, H. K. Hinssen, et al., 'Oxidation behaviour of an HTR fuel element matrix graphite in oxygen compared to a standard nuclear graphite', *Nucl. Eng. Des.*, **vol. 227**, pp. 281–284, (2004).

[40] M. S. Seehra and A. S. Pavlovic, 'X-Ray diffraction, thermal expansion, electrical conductivity, and optical microscopy studies of coal-based graphites', *Carbon N. Y.*, **vol. 31**, no. 4, pp. 557–564, (1993).

[41] C. Karthik, J. Kane, et al., 'In situ transmission electron microscopy of electron-beam induced damage process in nuclear grade graphite', *J. Nucl. Mater.*, **vol. 412**, no. 3, pp. 321–326, (2011).

[42] J. Kane, C. Karthik, et al., 'Microstructural characterization and pore structure analysis of nuclear graphite', *J. Nucl. Mater.*, **vol. 415**, no. 2, pp. 189–197, (2011).

[43] M. Le Guillou, N. Toulhoat, et al., 'Thermal behavior of deuterium implanted into nuclear graphite studied by NRA', *Nucl. Instruments Methods Phys. Res. Sect. B Beam Interact. with Mater. Atoms*, **vol. 332**, pp. 90–94, (2014).

[44] G. Zheng, P. Xu, et al., 'Characterization of structural defects in nuclear graphite IG-110 and NBG-18', *J. Nucl. Mater.*, **vol. 446**, no. 1–3, pp. 193–199, (2014).

[45] T. Tanabe, K. Niwase, et al., 'On the characterization of graphite', *J. Nucl. Mater.*, **vol. 191–194**, pp. 330–334, (1992).

[46] T. D. Burchell and L. L. Snead, 'The effect of neutron irradiation damage on the properties of grade NBG-10 graphite', *J. Nucl. Mater.*, **vol. 371**, pp. 18–27, (2007).

[47] R. B. Briggs, 'Molten-Salt Reactor Program Semiannual Progress Report', ORNL-3282, (1962).

[48] R. J. Sheil, R. B. Evans, et al., 'Molten Salt-Graphite Compatibility Test. Results of Physical and Chemical Measurement', ORNL-CF-59-8-133, (1959).

[49] Z. He, L. Gao, et al., 'Molten FLiNaK salt infiltration into degassed nuclear graphite under inert gas pressure', *Carbon N. Y.*, **vol. 84**, pp. 511–518, (2015).